CONFIDENTIAL

NACA

RESEARCH MEMORANDUM

PERFORMANCE OF SEVERAL HALF-CONICAL SIDE INLETS AT SUPERSONIC AND SUBSONIC SPEEDS

By Leonard E. Stitt, Robert W. Cubbison, and Richard J. Flaherty

Lewis Flight Propulsion Laboratory
Cleveland, Ohio

NATIONAL ADVISORY COMMITTEE FOR AERONAUTICS

WASHINGTON

February 1, 1956

CONFIDENTIAL

NATIONAL ADVISORY COMMITTEE FOR AERONAUTICS

RESEARCH MEMORANDUM

PERFORMANCE OF SEVERAL HALF-CONICAL SIDE INLETS AT SUPERSONIC AND SUBSONIC SPEEDS

By Leonard E. Stitt, Robert W. Cubbison, and Richard J. Flaherty

SUMMARY

An evaluation at Mach numbers of 2.0, 1.8, 1.5, and 0.65 of a series of half-conical side inlets mounted on the fuselage of a supersonic aircraft was made in the Lewis 8- by 6-foot supersonic tunnel. All the inlets were equipped with an internal flush slot for the removal of the compression-surface boundary layer and had provisions for fuselage boundary-layer removal. Provisions were made in the inlet system to use cones of different angles, two of them being single-angle cones of 25° and 30° and one, a double-angle cone of $25^{\circ} + 5^{\circ}$. All the inlets investigated had internal flush-slot bleed. A ducting system which would bypass air around the engine to an ejector was also investigated.

At free-stream Mach number 2.0 the maximum total-pressure recovery varied from 86.5 to 88 percent with approximately 6.5 percent bleed and 5 percent subcritical spillage. In general, the diffuser total-pressure distortions increased during both asymmetrical and yaw operation of the twin-duct system. The stable mass-flow range decreased significantly either with an increase in yaw angle or with a reduction in the boundary-layer diverter height.

INTRODUCTION

An investigation was conducted in the Lewis 8- by 6-foot supersonic wind tunnel to evaluate a series of half-conical side inlets mounted on a supersonic airplane. The performance characteristics of 25° half-angle cone inlets without throat bleed as well as with porous-surface and internal flush-slot bleed were reported in reference 1. This report covers the influence of variations in cone angle, of amount of fuselage boundary-layer removal, and of a bypass on the performance of inlets with flush-slot bleed near the throat.

SYMBOLS

The following symbols are used in this report:

A	area, sq ft
C_{D_a}	axial force coefficient, $\frac{D_a}{\frac{1}{2}\rho_0 v_0^2 A_f}$
D_a	axial force
D_s	bleed spillage drag
F_n	net thrust
$F_{n,i}$	ideal net thrust
h	distance between inboard cowl lip and fuselage
L	length of subsonic diffuser, 38.2 in.
M	Mach number
m^*	reference mass flow corresponding to choking at inlet throat at free-stream total pressure
$\frac{m_3}{m_0}$	engine mass-flow ratio, $\frac{\text{engine mass flow}}{\rho_0 v_0 A_i}$
$\frac{m_b}{m_0}$	total bleed mass-flow ratio, $\frac{\text{bleed mass flow}}{\rho_0 v_0 A_i}$
$\frac{m_e}{m_0}$	engine mass-flow ratio with bypass open
$\frac{m_i}{m_0}$	total inlet mass-flow ratio, $\frac{m_3 + m_b}{m_0}$
P	total pressure
p	static pressure
v	velocity

$\frac{W\sqrt{\theta}}{\delta A}$ corrected weight flow per unit area, lb/(sec)(sq ft)

x distance from cowl lip

α model angle of attack with respect to fuselage centerline

δ boundary-layer thickness

θ_l cowl-lip parameter

ψ model angle of yaw with respect to fuselage centerline

ρ mass density of air

Subscripts:

a axial

b bleed

e engine

f frontal

i inlet

x conditions at x distance from the cowl lip

0 free stream

3 diffuser-exit station

Pertinent areas:

A_e engine flow area with bypass installed, 0.127 sq ft

A_f maximum projected cross-sectional area, 0.663 sq ft

A_i total projected inlet cowl-lip area, sq ft

A_3 diffuser flow area, 0.161 sq ft

APPARATUS AND PROCEDURE

The installation of the one-sixth scale model in the tunnel is shown in figure 1. A sketch of the model (fig. 2) shows the details of the internal ducting, representative cross sections, and model dimensions. The twin half-conical side inlets were canted downward 4° with respect to the fuselage centerline, while the nose of the model was canted $2\frac{1}{2}^{\circ}$. The ducts were geometrically similar and joined into a common duct at model station 71.1. The engine and bleed mass flows were regulated by means of remotely controlled plugs (fig. 2).

Photographs and detailed sketches of the inlets are presented in figures 3 and 4, respectively. The cone was mounted on the fuselage and was undercut from its vertex to the cowl-lip station. This undercut was designed as part of the fuselage boundary-layer diverter system (fig. 4). In order to prevent the external boundary-layer air from entering the inlet system, the cowl was raised a constant height h off the fuselage. This distance was held constant by conforming the inboard cowl lip to match the body contour. The boundary-layer thickness ahead of the inlet was essentially constant (ref. 1) resulting in an inlet h/δ of either 1.50 or 1.04.

The faired fuselage axial force was determined by installing a pair of fairings in place of the inlets (figs. 3(d) and 4(f)). The inlet modifications included single half-angle cones of 25° and 30° and a double-angle cone of 25° + 5°. One configuration (fig. 4(a)) was investigated with and without undercut. Details of the internal flush-slot bleed were presented in reference 1. For the inlets presented here, the bleed-flow control plug was left in the full-open position.

The bypass was designed for a ratio of bypass area to engine area of 0.189. In the prototype, this system would supply the air for an ejector nozzle. In the model, the bypass was constructed by attaching a circular pipe to the sting simulating the engine as shown in figure 2. This system had its own total- and static-pressure instrumentation and mass-flow control plug.

The diffuser-area variation for the inlets, not including the bleed area, is presented in figure 5. Also shown is the area variation for the bypass system. Representative duct cross sections are also included.

Each inlet configuration will be designated as follows:

Configuration	Cone half angle, deg	Ratio of distance of inboard cowl lip from fuselage to boundary-layer height ahead of inlet, h/δ	Total projected inlet cowl-lip area, A_l, sq ft	Cowl-lip parameter, θ_l, deg
25-1.5-40	25	1.5	0.129	40
25-1.5-38	25	1.5	.151	38
30-1.5-45	30	1.5	.151	45
25+5-1.5-40	Double angle, 25+5	1.5	.129	40
25-1.04-40	25	1.04	.135	40

The internal strain gage used for the force measurements was such that only axial forces were obtained. The axial-force coefficient presented excludes the base pressure forces and the change in momentum from free stream to the exits of both main and bleed ducts. Other instrumentation and methods of data reduction are reported in detail in reference 1.

The investigation was conducted over a range of engine mass flows and angle of attack at Mach numbers of 2.0, 1.8, 1.5, and 0.65. The range of Reynolds number was approximately 4.1 to 5.3×10^6 per foot of length.

RESULTS AND DISCUSSION

The internal and external performance of the series of inlets investigated are presented for a range of engine mass-flow ratios in figure 6. A comparison of the various inlets at zero angle of attack is shown in figure 7. Mass-flow ratios greater than unity resulted from the use of the projected cowl-lip area as a reference (fig. 6). This procedure neglects the portion of the cone that extends from the inboard cowl lip to the fuselage. Lines of constant corrected weight flow are indicated on each of the internal-performance maps. The flagged symbols on figure 6 represent the lowest mass flow before static-pressure fluctuations greater than 5 percent of free-stream total pressure were noted. Hereinafter, this point will be considered as the minimum stable mass-flow point. For all the inlets presented herein, the bleed mass-flow control plugs were left in the full-open position. The change in bleed mass flow with engine mass flow was caused by the movement of the inlet terminal shock ahead of the bleed gap which changed the pressure ratio across the bleed system. The values plotted on the figures represent the sum of both bleed ducts.

At Mach numbers 2.0 and 1.8, the regions of decreasing pressure recovery at reduced engine mass flows primarily resulted from asymmetrical operation of the twin-duct system, for example, at engine mass-flow ratios less than 95 percent for Mach number 2.0 (fig. 6(a)). The fairings in the subcritical region were guided by static-pressure traces taken during transient operation of the mass-flow control plug. At Mach number 1.8, these traces indicated a sudden change in duct static pressure resulting in the sharp break of the mass-flow pressure-recovery curve (fig. 6(a)). For this condition, a sudden shift in the normal-shock location (one duct becoming supercritical and the other further subcritical) was also observed in the schlieren system at the break.

In general, the optimum performance of all the inlets was obtained at an angle of attack of 2°. This was expected since the inlets were alined with the local flow at this angle of attack (ref. 1). It was also noted that a slight decrease in performance resulted at an angle of attack of 5° and a significant decrease at an angle of attack of 10° in all cases.

The varying slope of the axial-force curves near critical operation was a result of a changing bleed mass flow; when the axial-force coefficient is plotted against total inlet mass flow (engine plus bleed mass flow) the curves have a constant slope. An increasing angle of attack resulted in a decrease in axial-force coefficient. The increase in minimum axial-force coefficient attained with the inlet configurations for decreasing Mach numbers (fig. 6) resulted from supercritical spillage drag associated with off-design operation.

In order to make a direct axial-force comparison, the inlet performance (fig. 7) was plotted against total inlet mass flow. This summary curve is presented for zero angle of attack, the only angle for which this comparison could be made. At Mach number 2.0, local Mach number 2.08 (ref. 1), peak total-pressure recovery of 88 percent was obtained with 5 percent normal-shock spillage and approximately 7 percent bleed. A variation of approximately 1.5 percentage points occurred between the inlets at all Mach numbers. Symmetrical twin-duct operation at Mach number 2.0 was limited to a small inlet-mass-flow range. Generally, the range of symmetrical operation increased with decreasing Mach numbers. Inlet 25-1.04-40 had the smallest stable operating range of the inlets investigated, indicating that decreasing h/δ had an adverse effect on this type of inlet. This was also indicated in reference 2.

In order to more realistically evaluate an inlet, the drag as well as pressure recovery must be considered. The effective thrust ratios at zero angle of attack for the inlets of this report are shown in figure 8. The curves represent the maximum obtainable thrust minus drag from each inlet over its mass-flow range and over the range of supersonic Mach

numbers. It should be pointed out that no attempt was made to size these inlets to any particular engine. However, the ratio of net thrust to ideal net thrust, as well as ideal net thrust, was obtained from the performance of a present-day engine for an altitude of 35,000 feet. The additive drag ΔD_a is the increment of drag measured from the minimum value (fig. 7). The drag associated with the bleed air D_s was calculated with the assumption that the sonic discharge was parallel to the free-stream direction and may be pessimistic because of the low bleed recovery. Inlet 25-1.04-40 was the optimum configuration for the Mach number range below a value of 1.9 because of lower ΔD_a. The decrease at Mach number 2.0 was due to the slightly lower peak-pressure recovery. Although inlet 25-1.5-40 (without undercut) is slightly less efficient than inlet 25-1.04-40 over most of the Mach number range, its stable operating range was considerably greater. The effective thrust ratios of inlets 30-1.5-45 and 25+5-1.5-40 were lower because of higher additive drag at nearly the same peak-pressure recovery.

The most significant effect with increasing angle of yaw (fig. 9) was the decrease in stable mass-flow range. Increasing the angle of yaw from zero to 6° for inlet 25-1.5-38 resulted in a decrease of 36 percentage points of stable mass-flow range at Mach number 2.0, corresponding to an 88 percent reduction. A similar decrease in inlet stability is also shown in references 3 and 4. Yaw operation of a twin-duct inlet system can also be expected to produce adverse effects on the diffuser-exit profiles (refs. 3 and 4). These contours for inlet 25-1.5-38 are shown over the Mach number range for both zero and 6° angle of yaw in figure 10. Generally, the shape of the windward contours remained the same; however, in all cases the maximum distortion increased as the angle of yaw increased. The maximum distortion, defined as the ratio of the difference between maximum and minimum total-pressure recovery to the duct average, was obtained directly from the profiles and do not necessarily appear on the contours. Typical total-pressure distributions over the range of angle of attack and mass-flow ratio are presented in reference 1. It was also shown that the maximum distortion increased during asymmetrical operation.

A comparison of the minimum axial-force coefficient for each configuration with the faired fuselage is presented in figure 11 for the range of supersonic Mach numbers. The larger increases at the lower Mach numbers were due to oblique-shock spillage drag associated with off-design operation. Increasing the maximum body cross-sectional area by 6 percent with inlet 30-1.5-45 resulted in the largest increase in C_{D_a}. The smallest increases above the faired fuselage were obtained with inlet 25-1.04-40.

A particular bypass system, designed to pass air through a fixed area around the engine to an ejector, was investigated with inlet 25-1.5-40. The pressure ratio across the fixed bypass area was sufficient to

ensure a choked exit at all times. The internal performance (fig. 12) indicates that reduced engine mass flows could be obtained without a change in critical and peak total-pressure recovery. The bypassed mass flow varied from 20 to 25 percentage points over the range of Mach numbers. Had a variable-area bypass been used, various engine air-flow requirements could be satisfied while maintaining critical inlet operation. In a comparison of figures 12 and 6(a) asymmetrical flow operation is shown to occur at approximately the same value of corrected engine weight-flow. The shift in corrected weight flow with bypass is a result of using engine area instead of total diffuser area as a reference.

The internal performance of inlet 25-1.5-40 (with undercut) at a free-stream Mach number of 0.65 (fig. 13) is representative of all the inlets. In this figure, m^* is a reference mass flow and is defined as the value corresponding to choking at the inlet throat area at free-stream total pressure. The performance agrees closely with the theoretical results obtained for sharp-lipped inlets at subsonic Mach numbers (ref. 5).

SUMMARY OF RESULTS

An investigation was conducted in the Lewis 8- by 6-foot supersonic wind tunnel to evaluate a series of half-conical side inlets mounted on a supersonic aircraft. These inlets included two single-angle cones of 25° and 30° and one double-angle cone of $25^\circ+5^\circ$. All the inlets investigated had internal flush-slot bleed. The following results were obtained:

1. Maximum total-pressure recovery obtained at free-stream Mach number 2.0 varied from 86.5 to 88 percent, with approximately 6.5 percent bleed and 5 percent subcritical spillage.

2. Asymmetrical operation of the twin-duct system occurred at reduced engine mass flows for Mach numbers of 2.0 and 1.8.

3. An 88 percent reduction in stable mass-flow range and an increase in distortion occurred as the angle of yaw was increased from zero to 6° at free-stream Mach number 2.0.

4. A decrease in the boundary-layer diverter height reduced the stable mass-flow range significantly at Mach numbers of 2.0 and 1.8.

5. For a particular bypass system, a reduction of 20 to 25 percentage points in engine mass flow was obtained at critical inlet operation without a change in internal performance.

Lewis Flight Propulsion Laboratory
National Advisory Committee for Aeronautics
Cleveland, Ohio, October 12, 1955

REFERENCES

1. Stitt, Leonard E., McKevitt, Frank X., and Smith, Albert B.: Effect of Throat Bleed on the Supersonic Performance of a Half-Conical Side-Inlet System. NACA RM E55J07, 1955.

2. Piercy, Thomas G., and Johnson, Harry W.: A Comparison of Several Systems of Boundary-Layer Removal Ahead of a Typical Conical External-Compression Side Inlet at Mach Numbers of 1.88 and 2.93. NACA RM E53F16, 1953.

3. Obery, Leonard J., and Stitt, Leonard E.: Investigation at Mach Numbers 1.5 and 1.7 of Twin-Duct Side Air-Intake System with 9° Compression Ramp Including Modifications to Boundary-Layer-Removal Wedges and Effects of a Bypass System. NACA RM E53H04, 1953.

4. Obery, Leonard J., Stitt, Leonard E., and Wise, George A.: Evaluation at Supersonic Speeds of Twin-Duct Side-Intake System with Two-Dimensional Double-Shock Inlets. NACA RM E54C08, 1954.

5. Fradenburg, Evan A., and Wyatt, DeMarquis D.: Theoretical Performance Characteristics of Sharp-Lip Inlets at Subsonic Speeds. NACA Rep. 1193, 1954. (Supersedes NACA TN 3004.)

Figure 1. - Model in tunnel.

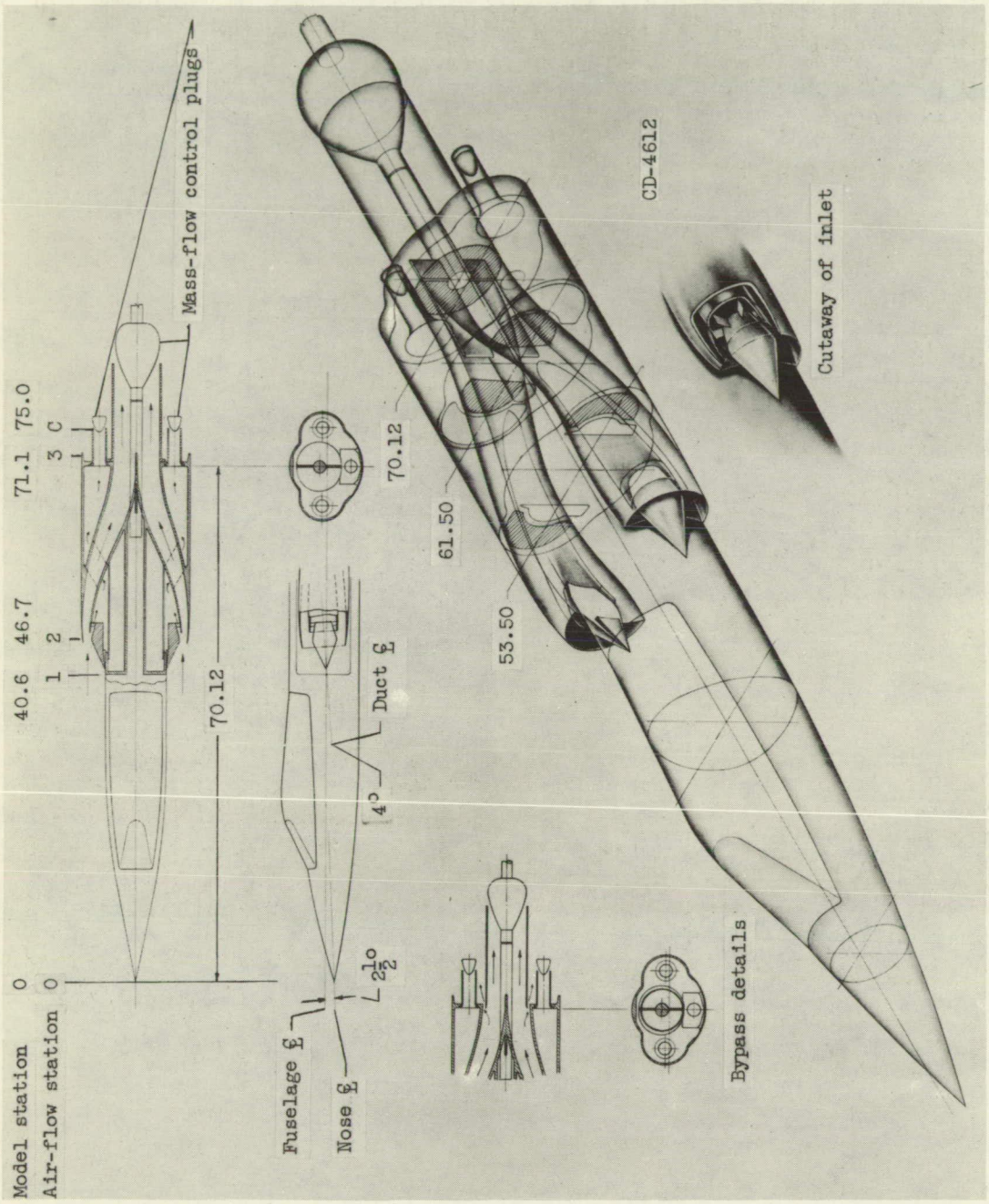

Figure 2. - Sketch of model. (All dimensions in inches except as noted.)

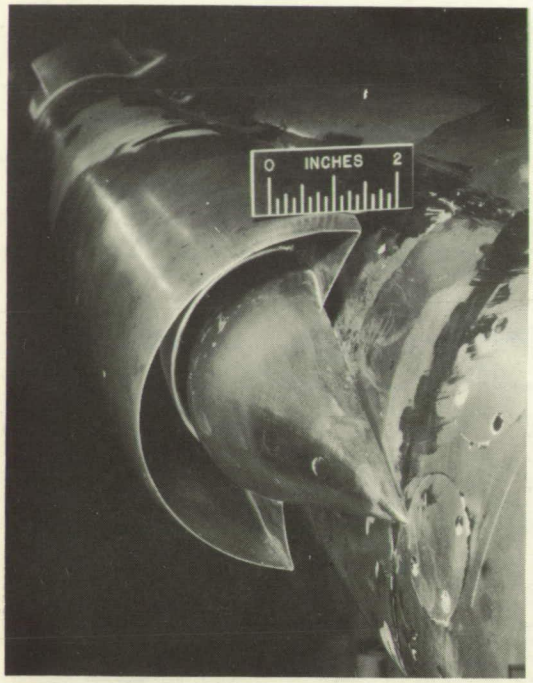

(a) Inlet 25-1.5-40.

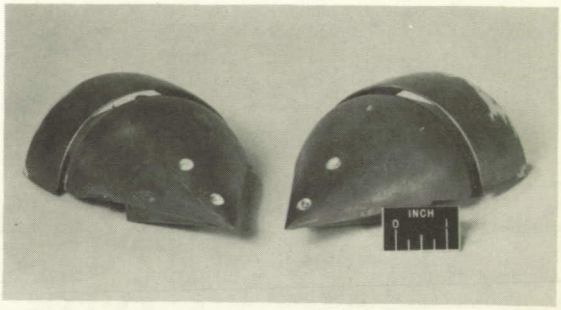

(b) 30° cone.

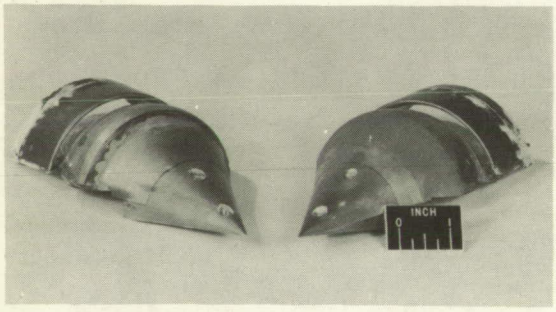

(c) 25°+5° double-angle cone.

(d) Faired-duct configuration.

Figure 3. - Inlets with modifications.

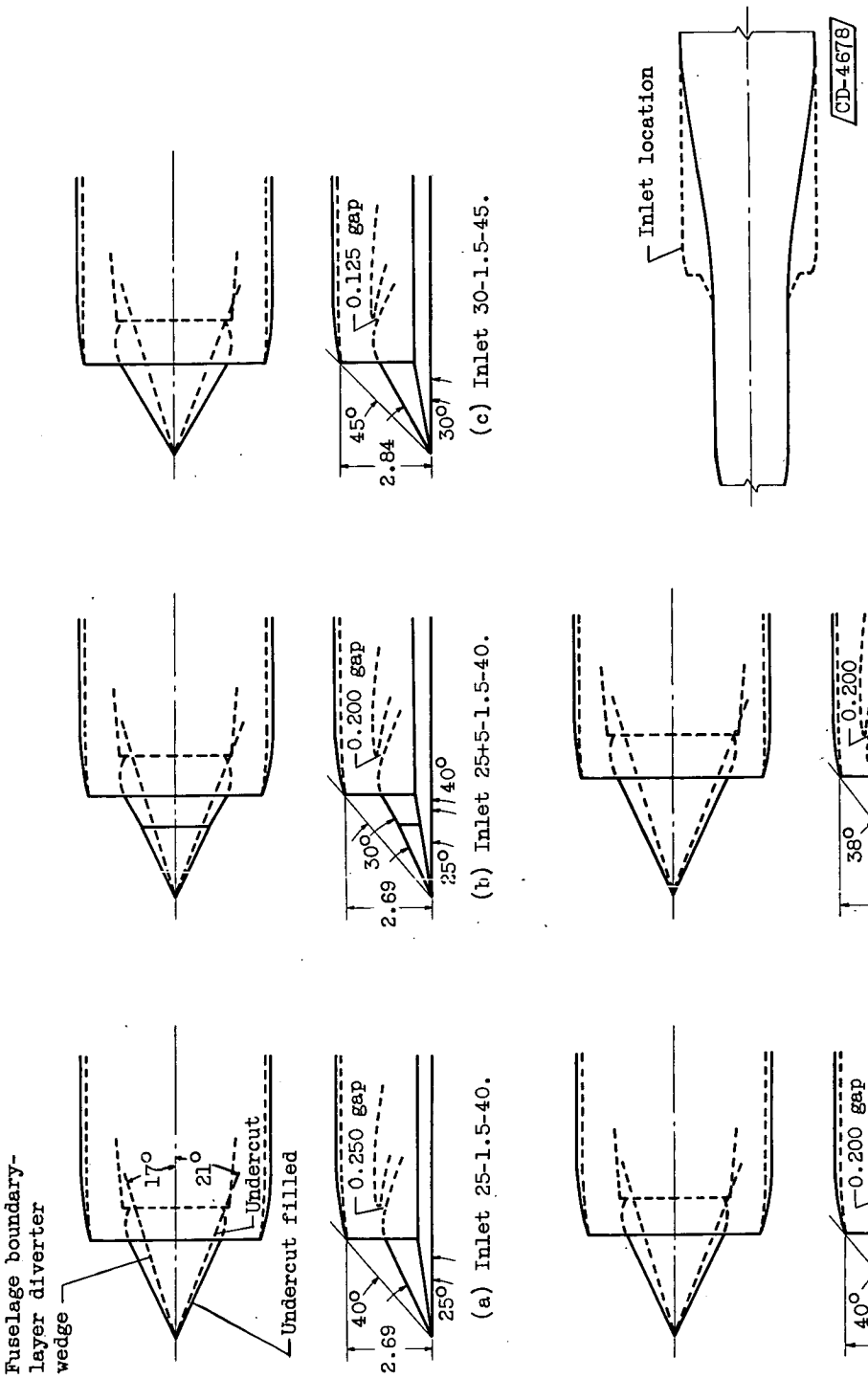

(a) Inlet 25-1.5-40.

(b) Inlet 25+5-1.5-40.

(c) Inlet 30-1.5-45.

(d) Inlet 25-1.04-40.

(e) Inlet 25-1.5-38.

(f) Faired fuselage configuration.

Figure 4. - Detailed sketches of the inlet configurations. (All dimensions in inches except as noted.)

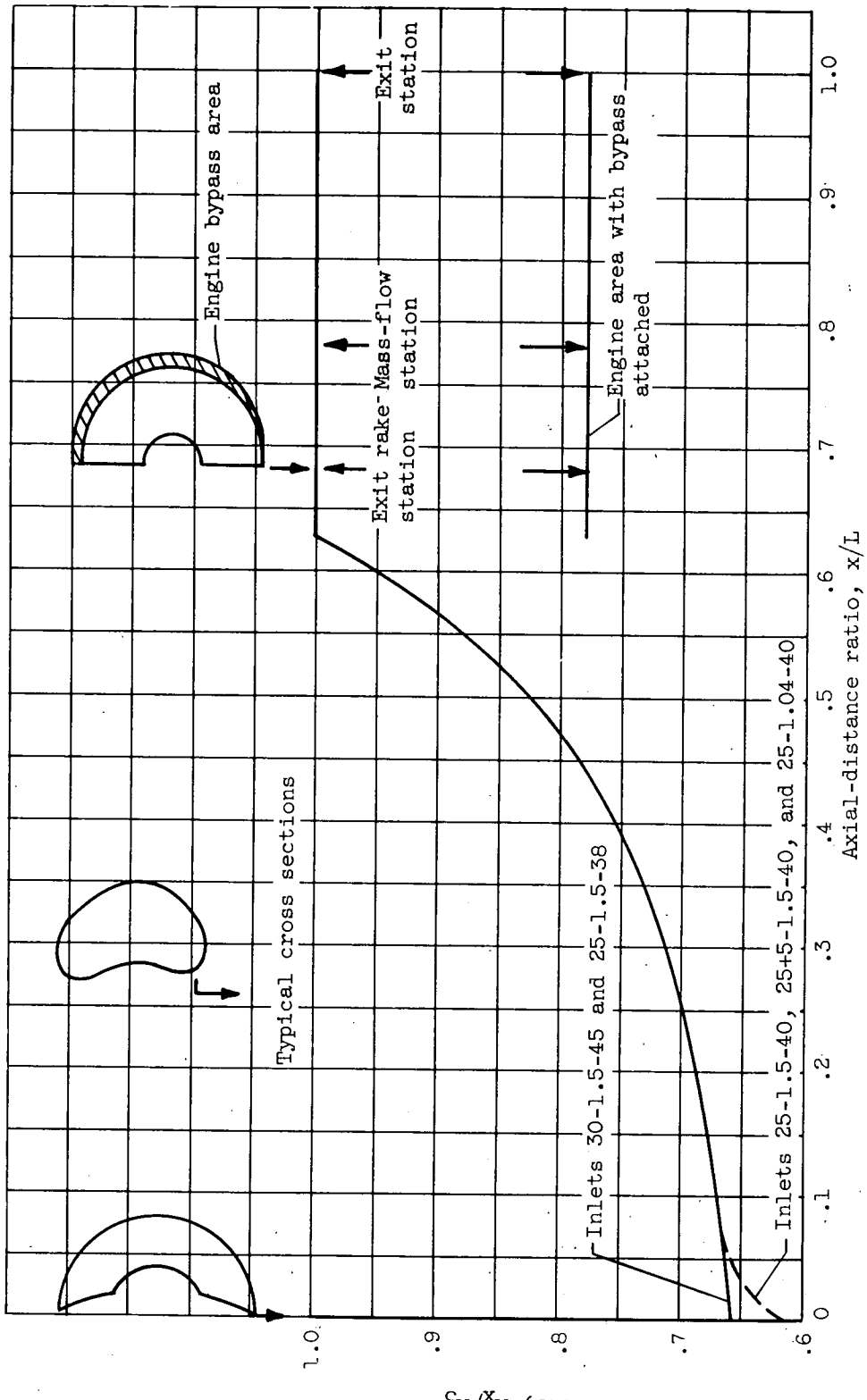

Figure 5. - Subsonic-diffuser area variation.

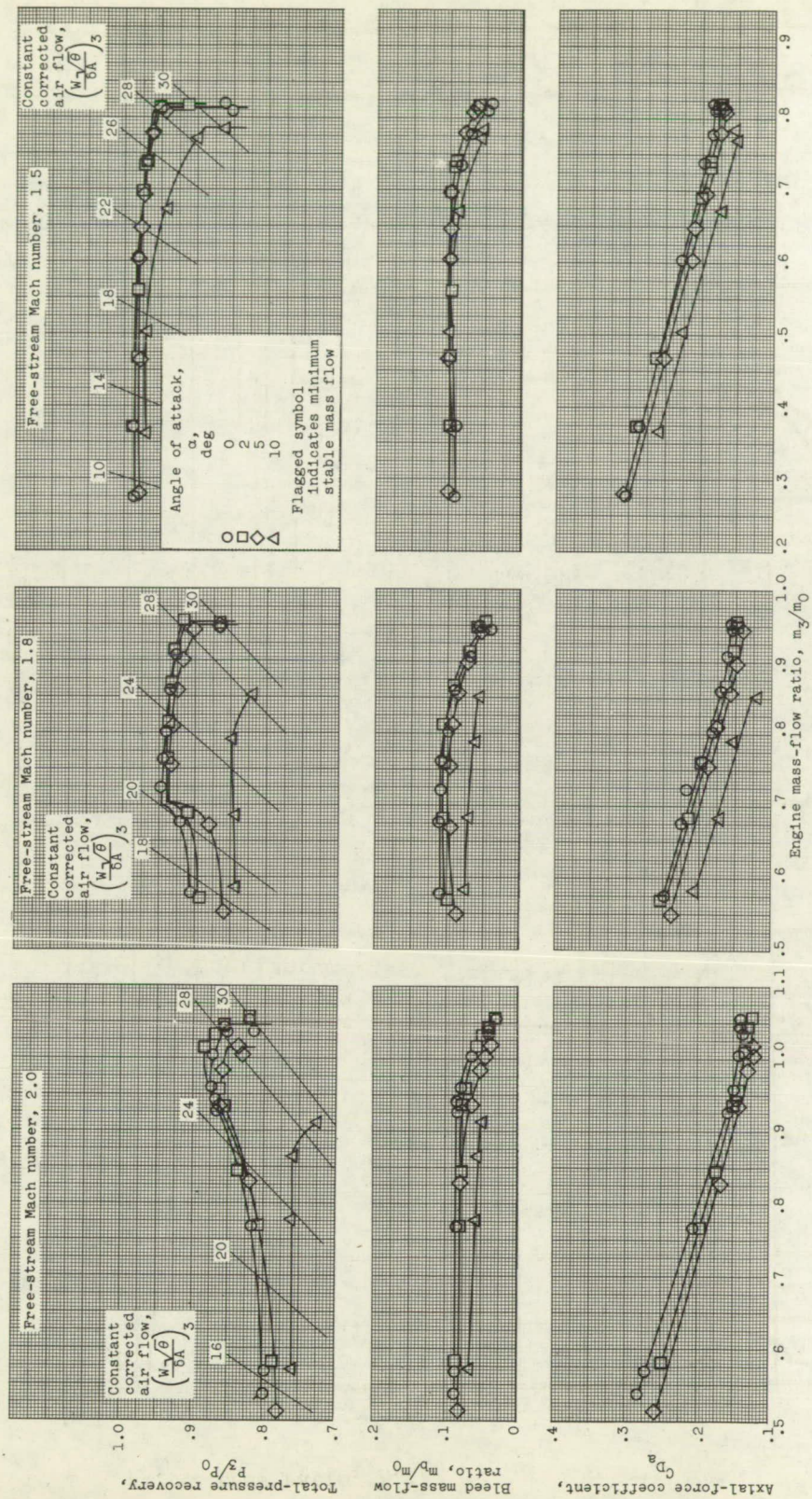

(a) Inlet 25-1.5-40; undercut filled.

Figure 6. - Inlet performance.

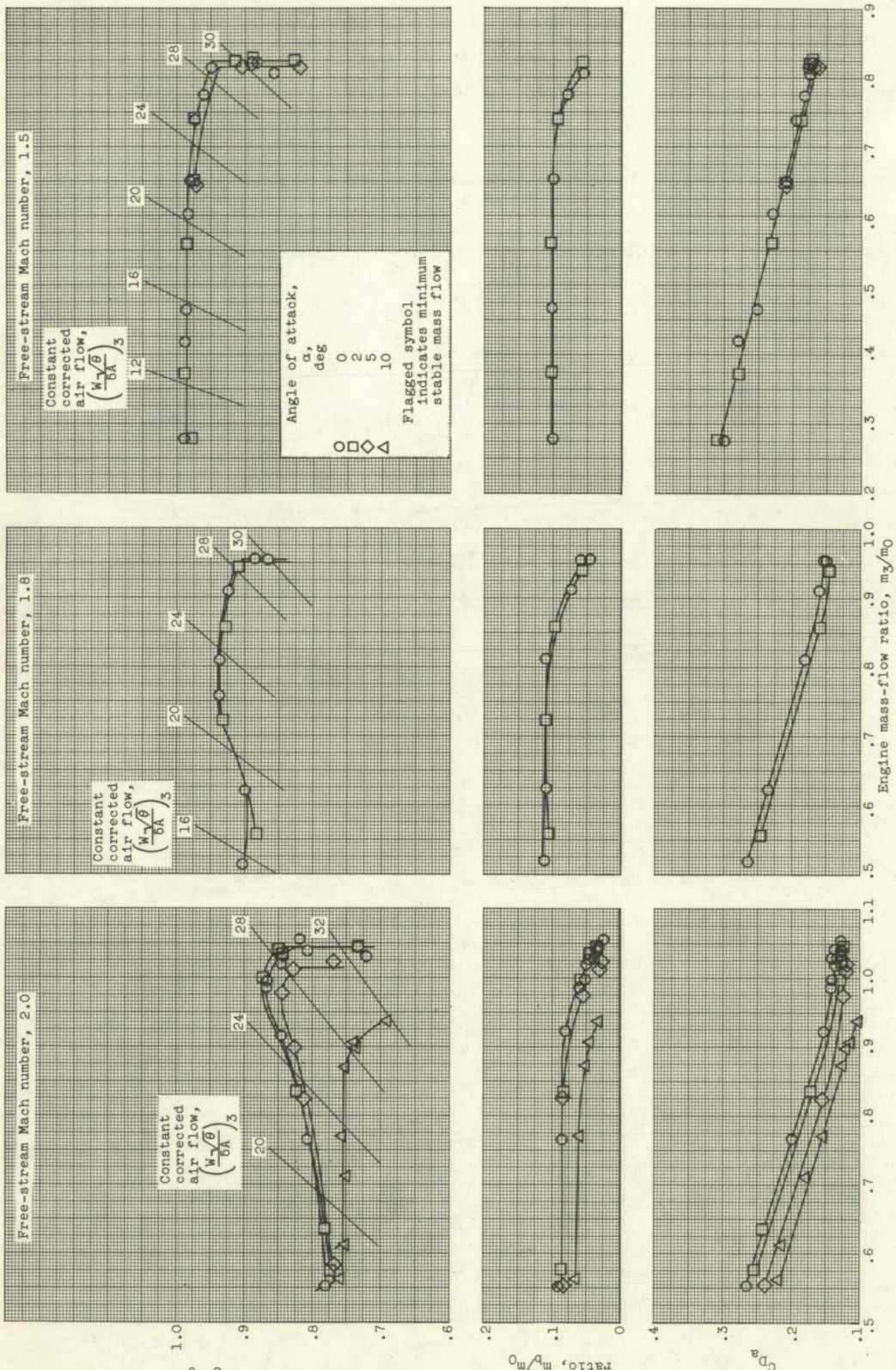

(b) Inlet 25-1.5-40; with undercut.

Figure 6. - Continued. Inlet performance.

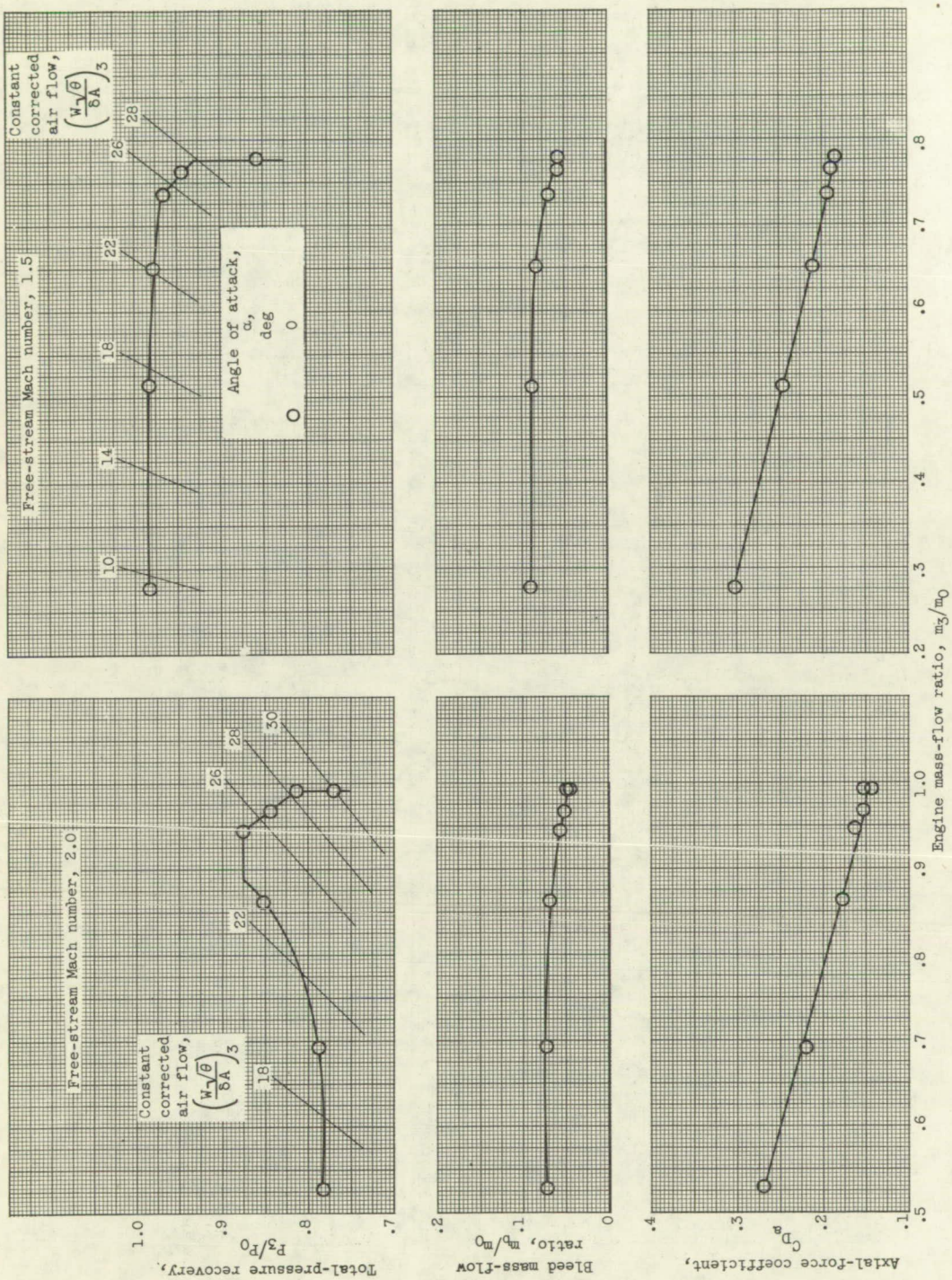

(c) Inlet 2545-1.5-40; with undercut.

Figure 6. - Continued. Inlet performance.

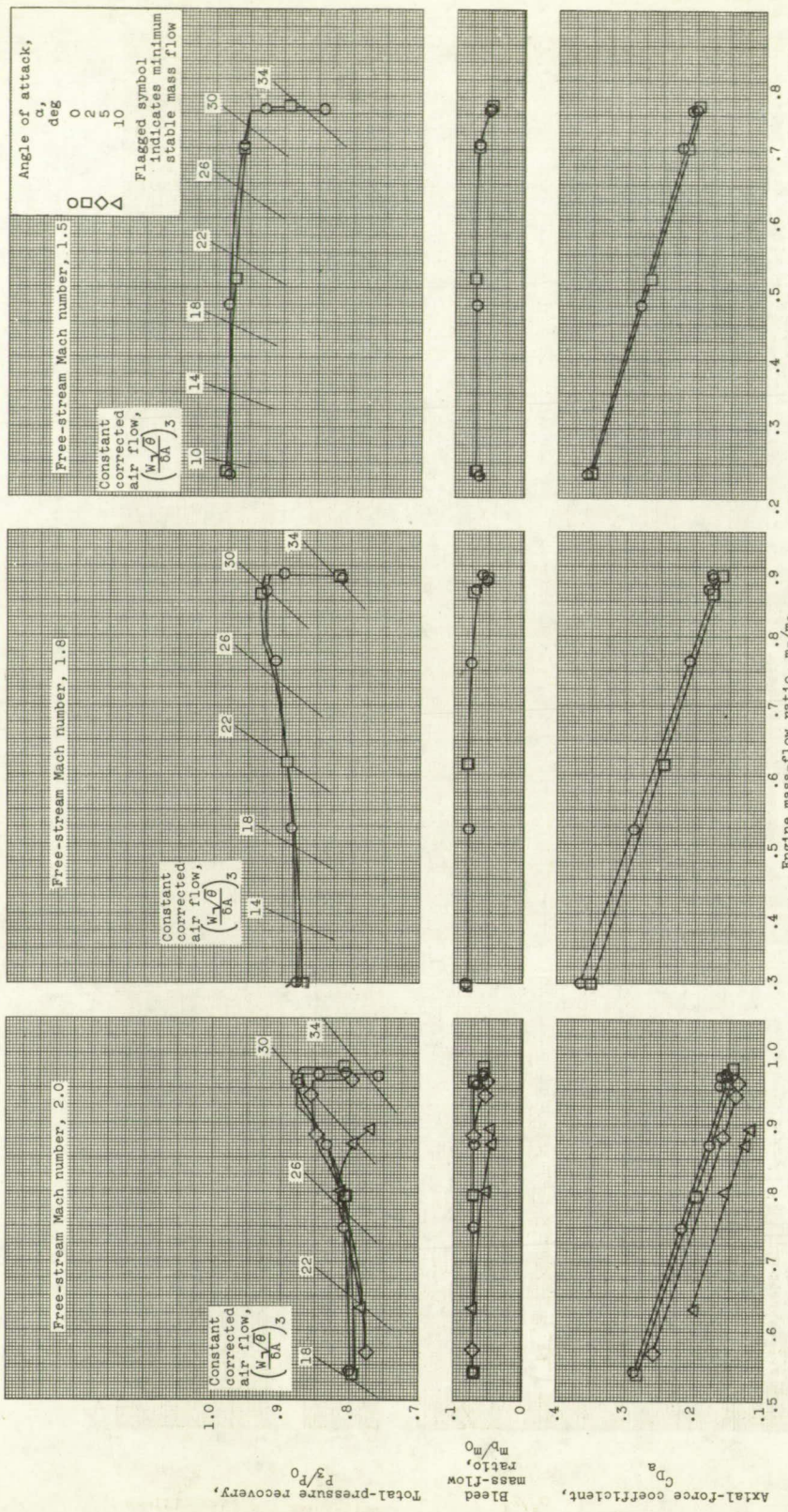

(d) Inlet 30-1.5-45; with undercut.

Figure 6. - Continued. Inlet performance.

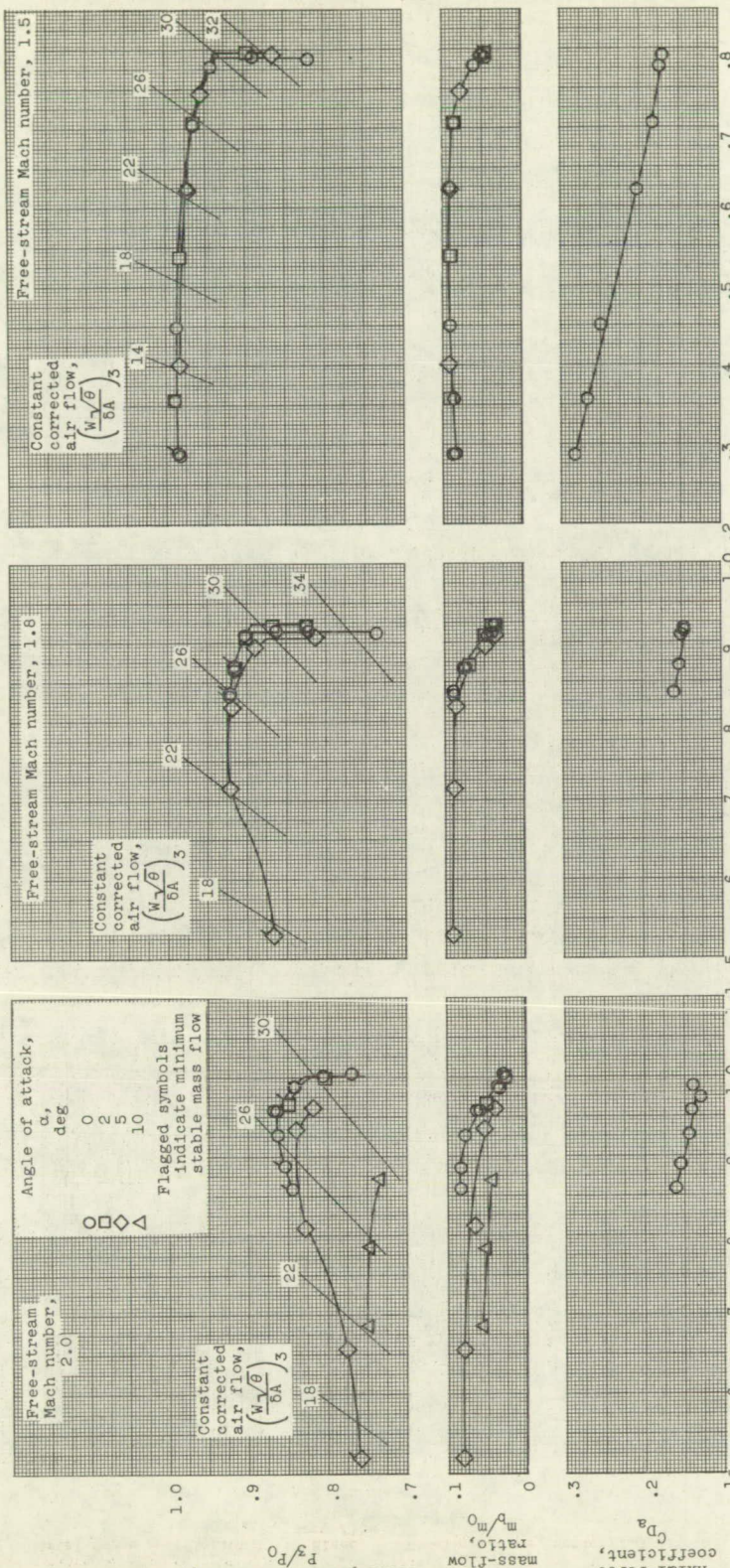

(e) Inlet 25-1.04-40; with undercut.

Figure 6. - Concluded. Inlet performance.

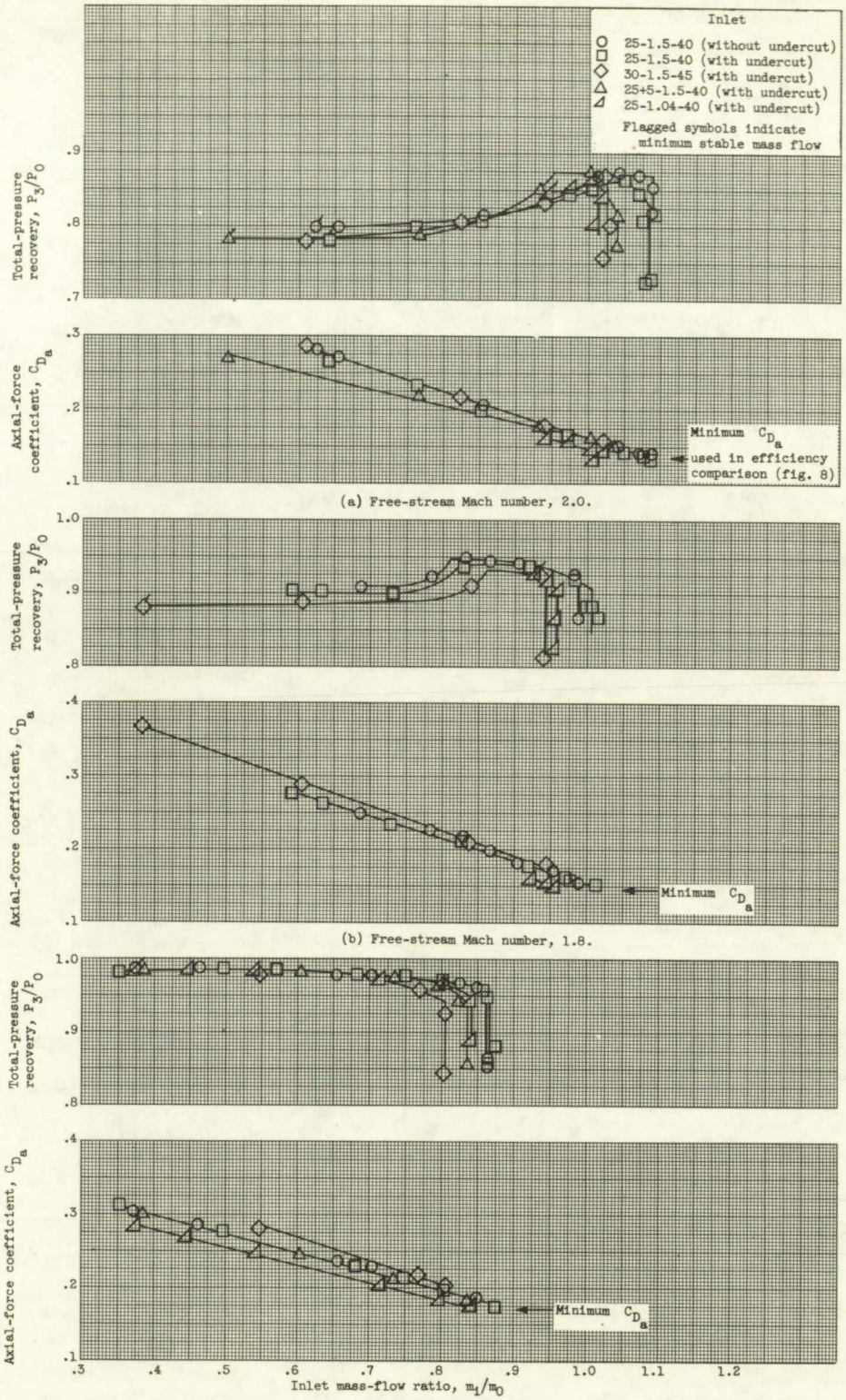

(a) Free-stream Mach number, 2.0.

(b) Free-stream Mach number, 1.8.

(c) Free-stream Mach number, 1.5.

Figure 7. - Comparison of various configurations at zero angle of attack.

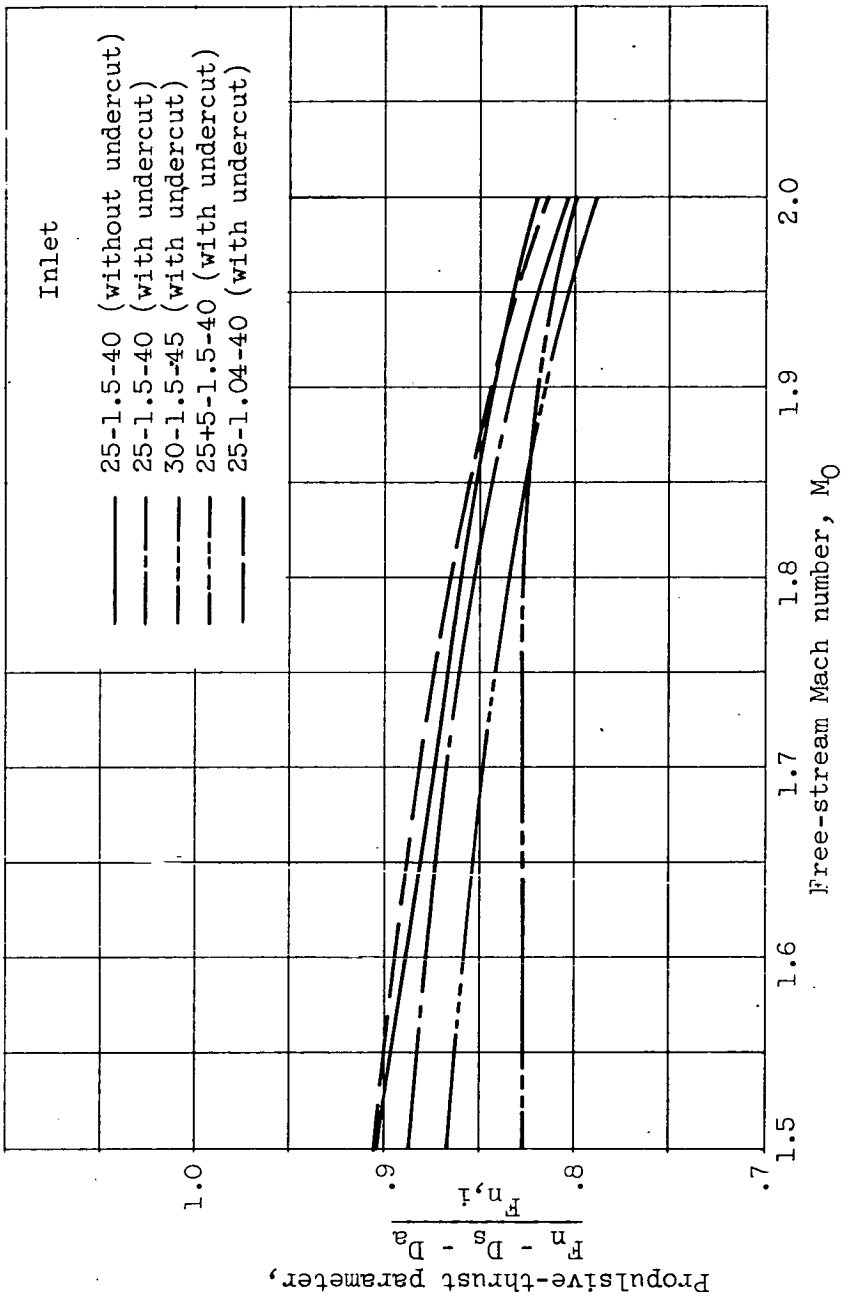

Figure 8. - Inlet comparison at an altitude of 35,000 feet and zero angle of attack.

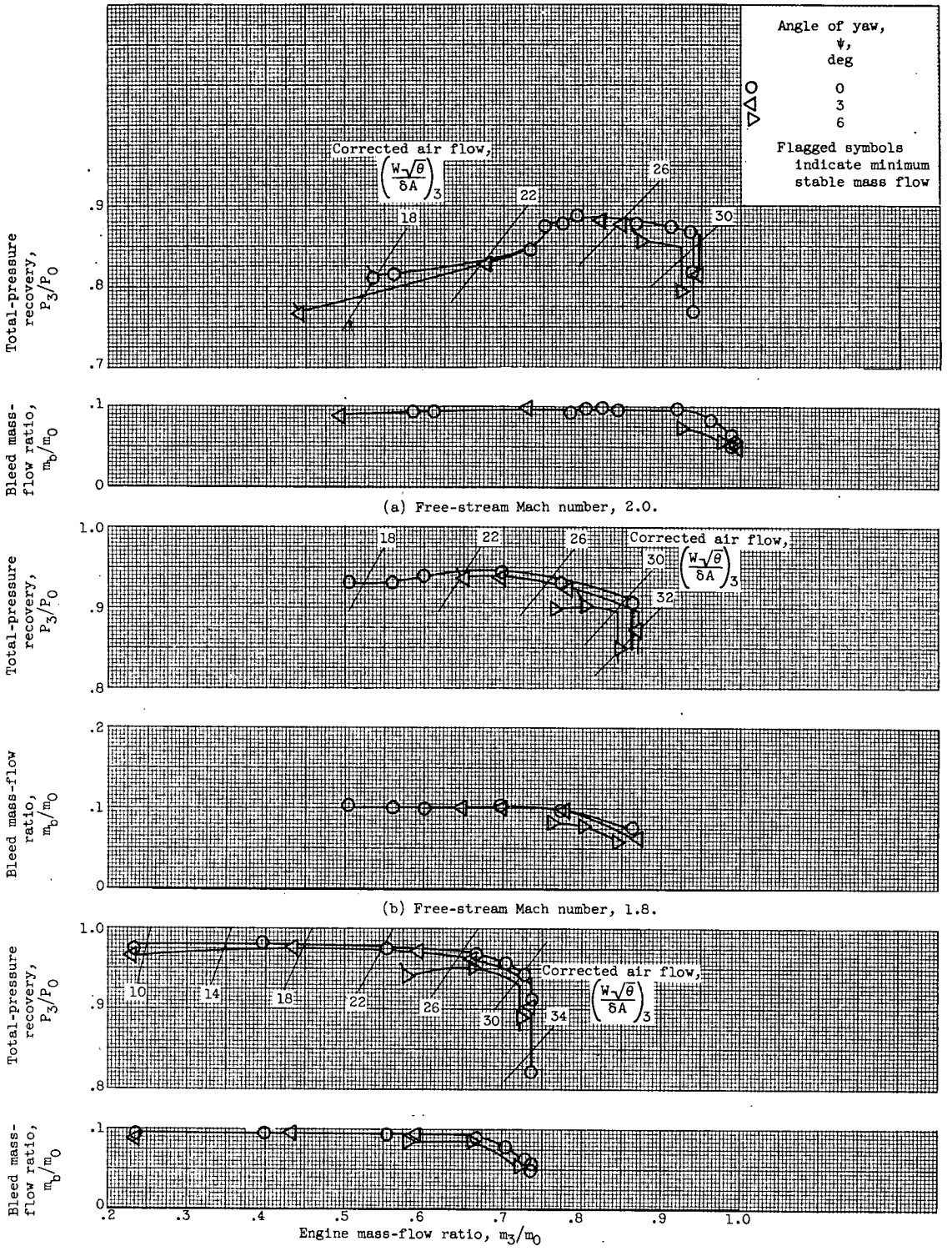

(a) Free-stream Mach number, 2.0.

(b) Free-stream Mach number, 1.8.

(c) Free-stream Mach number, 1.5.

Figure 9. - Performance of inlet 25-1.5-38 in yaw.

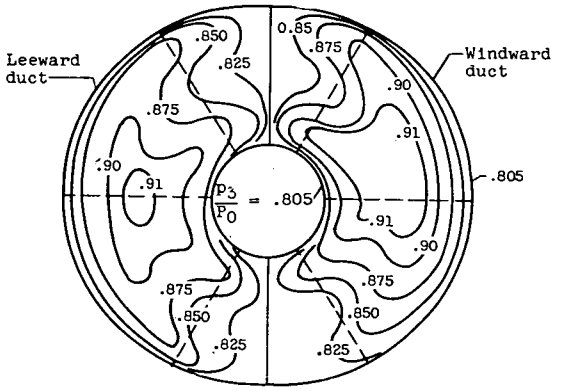

(a) $M_0 = 2.0$; $\psi = 0^\circ$; $m_3/m_0 = 0.91$; $P_3/P_0 = 0.875$; maximum distortion, 11.9 percent.

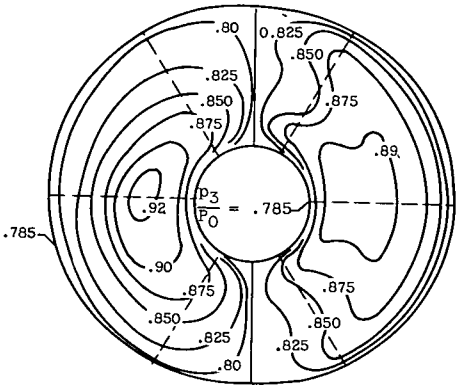

(b) $M_0 = 2.0$; $\psi = 6^\circ$; $m_3/m_0 = 0.872$; $P_3/P_0 = 0.857$; maximum distortion, 15.4 percent.

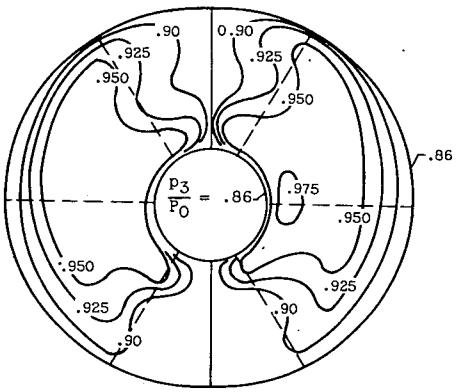

(c) $M_0 = 1.8$; $\psi = 0^\circ$; $m_3/m_0 = 0.773$; $P_3/P_0 = 0.932$; maximum distortion, 10.9 percent.

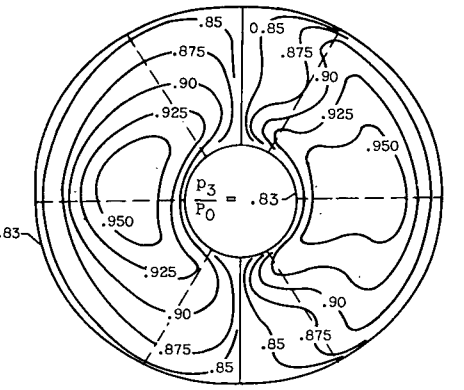

(d) $M_0 = 1.8$; $\psi = 6^\circ$; $m_3/m_0 = 0.764$; $P_3/P_0 = 0.900$; maximum distortion, 13.4 percent.

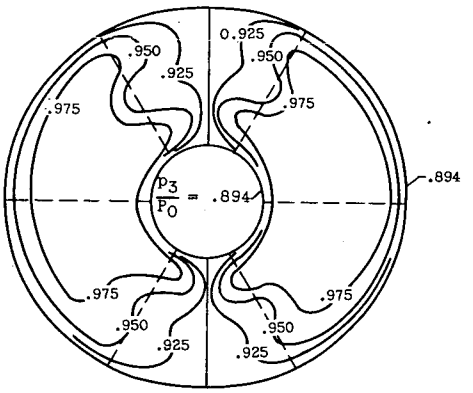

(e) $M_0 = 1.5$; $\psi = 0^\circ$; $m_3/m_0 = 0.666$; $P_3/P_0 = 0.967$; maximum distortion, 8.3 percent.

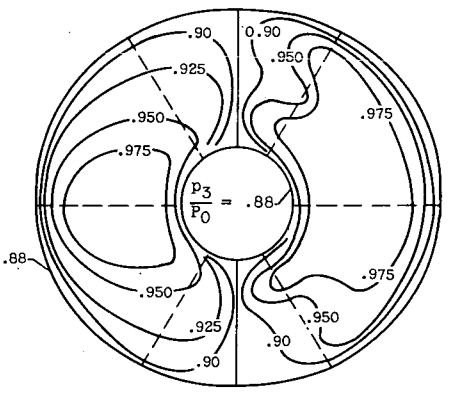

(f) $M_0 = 1.5$; $\psi = 6^\circ$; $m_3/m_0 = 0.659$; $P_3/P_0 = 0.951$; maximum distortion, 11.3 percent.

Figure 10. - Diffuser-exit total-pressure contours of inlet 25-1.5-38 (with undercut) in yaw.

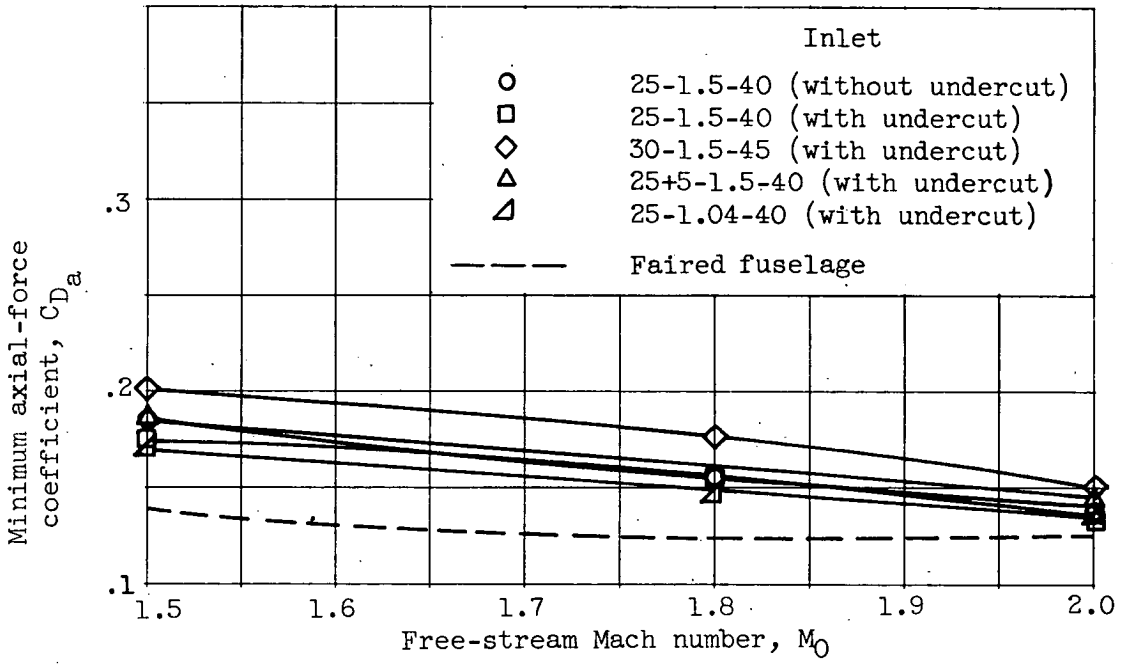

Figure 11. - Increase in drag due to addition of inlets; zero angle of attack.

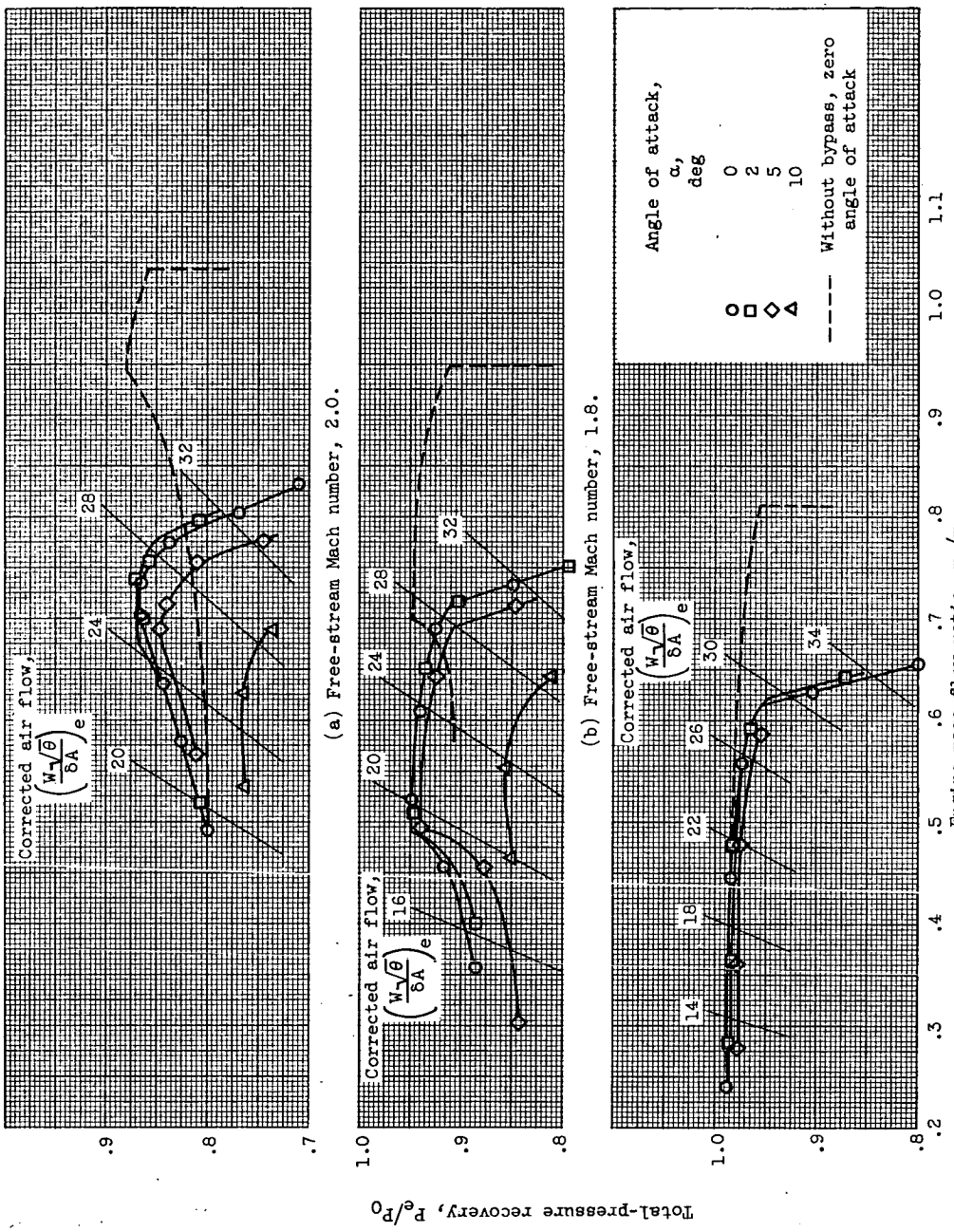

Figure 12. - Performance of inlet 25-1.5-40 with engine bypass.

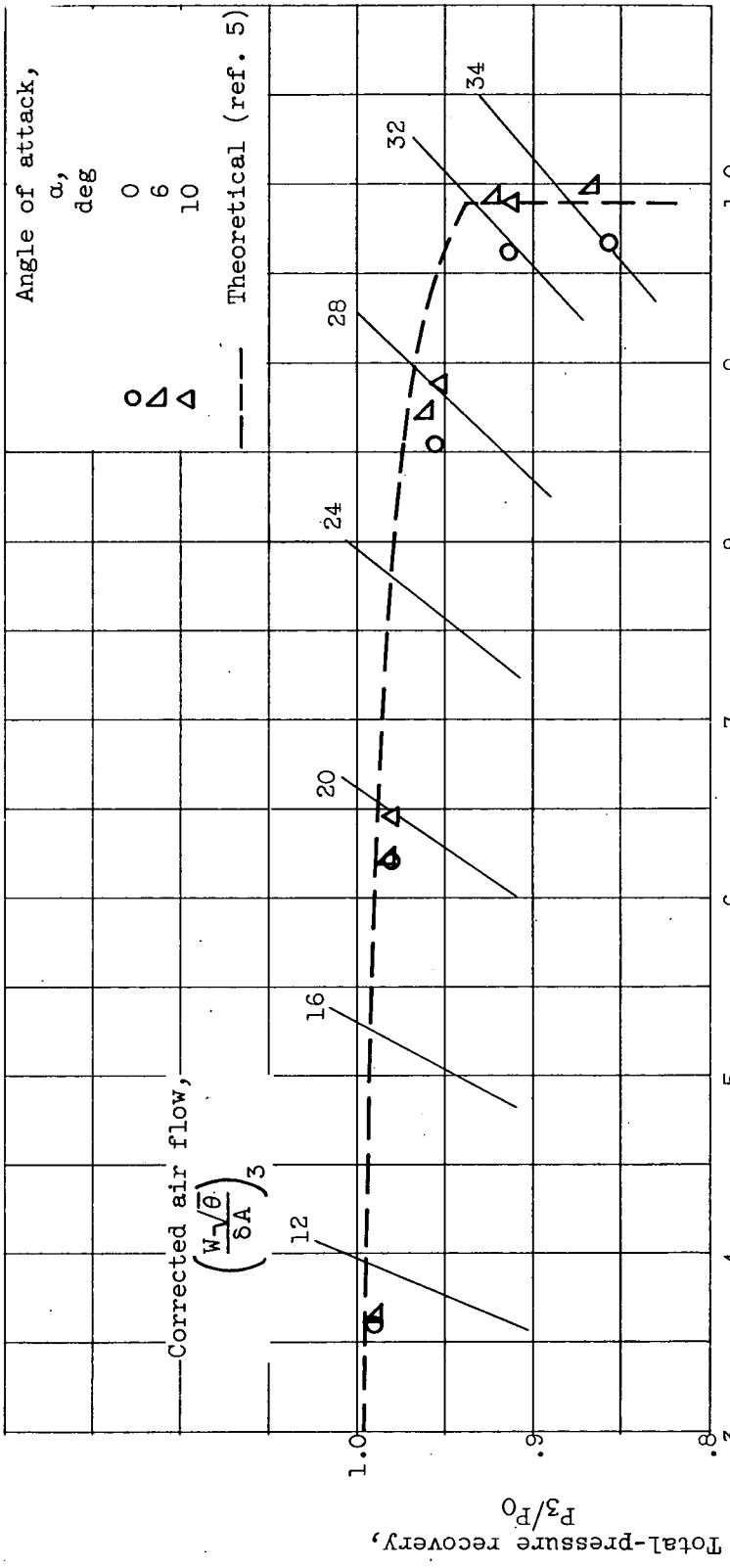

Figure 13. - Internal performance of inlet 25-1.5-40 (with undercut) at free-stream Mach number, 0.65.

NACA - Langley Field, Va.